NISTIR 7134

Submillimeter and Thz Detection of Dimethyl Methyl Phosphate in Air

Vyacheslav B. Podobedov
Richard Lavrich
Timothy M. Korter
Gerald T. Fraser
David F. Plusquellic

U. S. DEPARTMENT OF COMMERCE
Technology Administration
National Institute of Standards
and Technology
Optical Technology Division
Physics Laboratory
Gaithersburg, MD 20899

Alan C. Samuels

Passive Standoff Detection Group
Edgewood Chemical and Biological Center
Edgewood Area
Aberdeen, MD 21010-5424

July 2004

U.S. DEPARTMENT OF COMMERCE
Donald L. Evans, Secretary

TECHNOLOGY ADMINISTRATION
Phillip J. Bond, Under Secretary for Technology

NATIONAL INSTITUTE OF STANDARDS
AND TECHNOLOGY
Arden L. Bement, Jr., Director

Abstract

Experimental measurements and theoretical calculations were performed to assess the potential for using continuous-wave submillimeter and THz (far-infrared) linear-absorption spectroscopies to detect chemical-warfare agents in air at ambient temperatures and pressures. The experimental studies used three different instruments: a far-infrared, Fourier-transform, polarizing interferometer; a frequency-stabilized, backward-wave oscillator (BWO); and a near-infrared, laser-pumped, THz photomixer. The sensors were evaluated on dimethyl methyl phosphonate (DMMP, $C_3H_9O_3P$), a common simulant for nerve agents. Recommendations are provided for improving submillimeter and far-infrared methods for the detection of chemical-warfare agents.

I. Introduction

There is a continued interest in new optical methods for the detection and quantification of chemical-warfare agents in air for homeland and military defense as no single instrument offers the desired universal, rapid, unambiguous, and sensitive detection and high-accuracy quantification of these agents under all environmental conditions. Because of the wide range of chemical and physical properties (vapor pressure, electric dipole moment, infrared band strengths, etc.) of the agents, optical methods differ in their utility for the detection of a particular agent or class of agents. Some of the desired characteristics of an optical sensor for agent detection include:

- Ability to unambiguously identify a chemical agent
- High sensitivity and rapid response to allow early detection of a chemical-agent release to ensure that adequate protective measures can be taken
- Poor atmospheric transmission when recognition by a foe is undesirable and excellent atmospheric transmission for early-warning standoff sensors
- Insensitivity to heat and humidity level to allow operation under all weather conditions and in tropical and desert regions
- Technical simplicity to ensure reliable operation by minimally trained users
- Immunity to chemical camouflaging and to interference from atmospheric gases and common urban, agricultural, and battlefield pollutants
- Low cost to allow wide use

In the present report we examine the potential of continuous-wave (cw) submillimeter-wavelength and far-infrared or terahertz methods for the detection of chemical-warfare agents in air. These methods probe the rotational and torsional spectra of chemical agents, whereas the mid-infrared methods probe their vibrational spectra. Here, we operationally define the submillimeter region to be between 200 GHz and 800 GHz (6.7 cm^{-1} and 27 cm^{-1} or 1.49 mm and 0.37 mm) and the far-infrared and THz region to be between 800 GHz and 4000 GHz (27 cm^{-1} and 400 cm^{-1} or 370 μm and 25 μm). Historically, the development of submillimeter and far-infrared methods for chemical sensing have been limited due to the instrumentation challenges present in this quasi-

optical regime and due to the strong, nearly continuous, atmospheric absorption above approximately 1 THz (33.3 cm^{-1}) , as illustrated in Fig. 1 below.

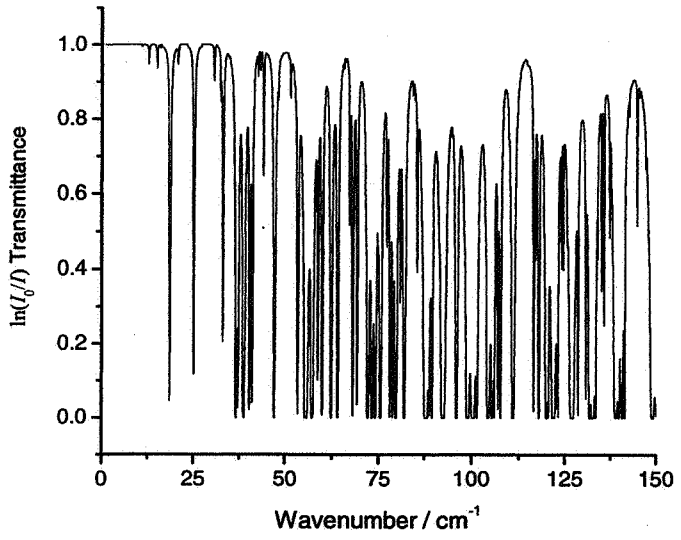

Fig. 1. Calculated transmittance spectrum for a U.S. standard atmosphere at a 1 m pathlength. The spectrum is dominated by the absorption from the 0.79 kPa (5.9 Torr) partial pressure of water.

Here, we address the detection of a model nerve agent, dimethyl methyl phosphonate (Fig. 2), using three types of submillimeter or THz spectrometers: a far-infrared, Fourier-transform, polarizing interferometer; a frequency-stabilized, backward-wave oscillator (BWO); and a near-infrared, laser-pumped, THz photomixer. The results from these studies are presented below following a brief discussion of the modeling of the submillimeter and THz spectrum of DMMP.

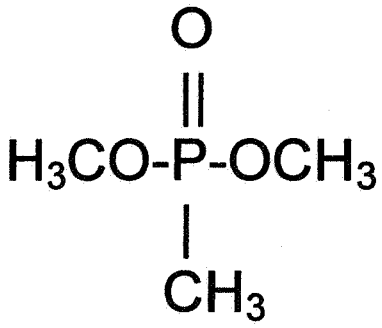

Fig. 2. Structure of dimethyl methylphosphonate

II. Spectral Modeling

The present effort is concerned with the detection of chemical-warfare agents using submillimeter and THz radiation. Of primary interest is the detection of the agents under ambient conditions, that is, as trace impurities in air at atmospheric pressure and near room temperature. In this section we present model calculations of the spectrum of DMMP under these conditions to estimate the magnitude of the fractional absorption of the submillimeter and THz radiation and the uniqueness of the shape of the spectral band

for agent identification, as specified by low-order central moments, M_n, of the absorption cross section, $\sigma(\nu)$, defined by the following equations:

$$M_0 = \int \sigma(\nu)\, d\nu$$

$$M_1 = \int \nu\, \sigma(\nu)\, d\nu \qquad (1)$$

$$M_{n>1} = \int (\nu - M_1)^n \sigma(\nu)\, d\nu\,,$$

where ν is the frequency. An alternative approach of using low-pressure gas samples with high-spectral-resolution submillimeter or THz sources to resolve individual rotational or rotational-tunneling lines for unambiguous agent identification is also considered. As we show below, this approach suffers from unacceptably poor sensitivity due to the large number of thermally populated rotational, vibrational, and conformational states of DMMP and most chemical agents, which limit the intensity available in any one spectral line for monitoring or detection purposes. Below, we separately discuss the model calculations as applied to the detection of DMMP in low-pressure and in atmospheric-pressure gas samples. Later, we will describe the validation of the calculations by experimental measurements. We are only concerned with the detection of pure rotation and rotation-tunneling spectra, and not the rotation-torsional spectra, which generally lie at higher frequencies and are not presently well predicted by *ab initio* quantum mechanical theories.

A. Low-Pressure Gas Samples

Low-pressure gas samples reduce or eliminate the effects from pressure or collisional line broadening, thus allowing the detection of individual rotational-tunneling transitions of DMMP. Indeed, with sufficient experimental sensitivity and spectral resolution, the frequencies of these lines can be measured to better than 0.1 MHz ($k = 2$ or 2σ). Measurements at this accuracy allow the unambiguous identification of a chemical agent based on the uniqueness of the line frequencies. Here, we consider first the ideal case in which the gas sample is pure DMMP. The detection sensitivity determined for this ideal case will furnish an upper bound for the detection sensitivity for DMMP in low-pressure samples of contaminated air where pressure broadening is small or negligible.

To undertake a modeling of the submillimeter and THz spectrum of DMMP, knowledge of the mean pressure broadening coefficient, rotational and vibrational partition functions, conformations, rotational constants, and electric-dipole moment components are required. These parameters will be used together with the spectral modeling program developed at the Jet Propulsion Laboratory by Pickett (1991) to simulate the DMMP submillimeter and THz spectrum to estimate the peak fractional absorption of the radiation by an individual rotational line, assuming the radiation source is spectrally narrow relative to the Doppler linewidth (0.56 MHz full width at half maximum (FWHM) at 500 GHz). In the present study, only the BWO source with its linewidth of less than 10 kHz is able to meet this criterion. The photomixer system has a linewidth of

3 MHz to 5 MHz, limited by pump-laser jitter, and the interferometer has a spectral resolution of 750 MHz (0.025 cm^{-1}).

The Doppler linewidth also sets the maximum desirable sample pressure for a high-resolution spectral investigation. To maximize the spectral resolution and sensitivity it is necessary to use sample pressures in which the pressure broadening contribution to the linewidth roughly matches the Doppler linewidth. At higher sample pressures, both the integrated intensity and the linewidth increase proportionally with the pressure, preventing any peak intensity gain and concomitant sensitivity gain from increasing the sample pressure. For pressures in which the collisional broadening contribution to the linewidth is less than the Doppler contribution, the peak and integrated signal intensities increase linearly with pressure.

The pressure broadening parameters are estimated to be on the order of 75 kHz/Pa (10 MHz/Torr) FWHM for air foreign-gas broadening and 375 kHz/Pa (50 MHz/Torr) FWHM for self-broadening, and are assumed to be independent of quantum state. Experimental pressure broadening measurements for molecules of this size are generally not available, although they are possible to estimate using Anderson's electrostatic model for collisional broadening (Townes and Schalow, 1955). The values chosen here are within the range of broadening coefficients found for other larger molecules, such as nitric acid, which has a broadening parameter of approximately 73 kHz/Pa for nitrogen broadening and 394 kHz/Pa for self broadening as measured near 683 GHz by Zu *et al.* (2002). Near the 320 GHz intensity maximum for DMMP spectrum, sample pressures of less than 0.48 Pa (3.6 mTorr) are required to maintain the maximum spectral resolution.

We note that individual rotational-tunneling lines may also be resolvable with the photomixer system with its 3 MHz to 5 MHz linewidth (FWHM). Assuming that this is true, then the maximum sensitivity for detection of a chemical agent is achieved when the pressure broadening width is of the same size as the instrumental linewidth, i.e., 13 Pa (100 mTorr) for a pure DMMP sample with a 5 MHz instrumental linewidth.

The other necessary spectroscopic information on DMMP is available from the theoretical and experimental study of Suenram *et al.* (2002) and from density-functional calculations performed as part of the present study. Suenram *et al.* reported experimental values for the *A*, *B*, and *C* rotational constants for the lowest energy conformer of DMMP from molecular-beam microwave spectroscopy and theoretical values for the other two low-energy conformations from correlated *ab initio* electron-structure calculations at the MP2/6-311++G** level. The theoretical calculations also furnish estimates of the relative zero-point energies of the three conformers, as 0 cm^{-1}, 170 cm^{-1}, and 602 cm^{-1} and of the electric dipole moment components, μ_a, μ_b, and μ_c, along the three principal inertial axes. Density functional calculations (B3LYP 6-31G*) were used to estimate vibrational partition functions, Q_{vib}.

Table I. Spectroscopic constants of DMMP used in the simulation of the submillimeter and THz spectra.

Conformer	Symmetry	E_{rel} (cm^{-1})	A (MHz)	B (MHz)	C (MHz)	μ_a (D)	μ_b (D)	μ_c (D)	Q_{vib}	Q_{rot}
I	C_1	0[a]	2829[b]	1972[b]	1614[b]	0.54[a]	0.65[a]	2.22[a]	1256	289233
II	C_s	170[a]	2534[a]	2118[a]	1610[a]	1.48[a]	1.64[a]	0[d]	2819	295250
III	C_1	602[a]	2567[a]	2112[a]	1672[a]	1.45[a]	2.74[a]	3.51[a]	815	299264

[a] MP2/6-311++G** calculation of Suenram, et al. (2002).
[b] Experimental value of Suenram et al. (2002).
[c] Dipole moment in Debye. 1 C·m = $2.99792458 \times 10^{29}$ D.
[d] Zero by symmetry.
[e] From density functional calculations (B3LYP 6-31G*) for $T = 298.15$ K.

Examination of the conformer energies and the vibrational partition functions give an estimate of the fraction of molecules in a sample which are in the ground vibrational state of the lowest energy conformer. This fraction is important in assessing the potential of the submillimeter and THz methods to detect and monitor individual rotational lines of chemical warfare agents. The conformer-vibrational partition function, $Q_{con\text{-}vib}$, is estimated from,

$$Q_{con\text{-}vib} = 2\, Q_{vib}^{I} + Q_{vib}^{II} \exp(-E_{II}/k_b T) + 2\, Q_{vib}^{III} \exp(-E_{III}/k_b T), \qquad (2)$$

under the assumption that only conformers I, II, and III are possible, i.e., are thermally populated, and that the rotational partition function, Q_{rot}, is effectively independent of vibrational and conformer state. That Q_{rot} varies little with conformer state, and presumably less so with vibrational state, can be seen in Table 1. In Eq. 1, k_b = 0.6950356 cm^{-1} K^{-1} is the Boltzmann constant, Q_{vib} is the vibrational partition function calculated in the harmonic approximation, and E_I, E_{II}, and E_{III}, are the relative conformer energies. Values for Q_{vib} and E_I, E_{II}, and E_{III} are listed in Table I. The factors of 2 in front of Q_{vib}^{I} and Q_{vib}^{III} are necessary to include the two enantiomers of these chiral conformers. We find that the fraction of molecules in a room temperature sample of DMMP in the ground vibrational and conformational state is $2\cdot(Q_{con\text{-}vib})^{-1}$ = 0.052 %, or $(Q_{con\text{-}vib})^{-1}$ = 0.026 % for each of the two enantiomers. The consequence of this large value of $Q_{con\text{-}vib}$ = 3842 for observing individual rotational lines is severe. For example, in 133 Pa (1 Torr) samples of HCN and of DMMP, approximately all of the HCN molecules will be in the ground vibrational-conformational state, whereas only 6.9 Pa (0.52 mTorr) of DMMP will be in this state, that is 3.5 Pa (0.26 mTorr) for each enantiomer.

In Fig. 3 we plot a stick spectrum of the individual lines, as predicted from the simulation program of Pickett. The calculation assumes that all the molecules reside in the ground vibrational state of the lowest energy conformer and was performed using the rotational constants and electric dipole moment components for conformer I listed in Table 1. The high line density is apparent in the figure from the near continuum nature of the plot, and is even greater when all the conformers, tunneling splittings, and thermally populated vibrational excited states are included. The spectrum consists of the 106067 lines which

result when levels up to $J = 400$, $K_a = 125$ are considered and an intensity cutoff of 10^{-7} MHz nm^2 is imposed on the integral absorption coefficient for the individual lines. We note that the rotational partition function resulting from a direct sum over the individual quantum states is 289,210 compared to the value of 289,233 obtained classically from,

$$Q_{rot} = \left[\frac{\pi}{ABC} \left(\frac{kT}{h} \right)^3 \right]^{1/2}, \qquad (3)$$

and listed in Table 1.

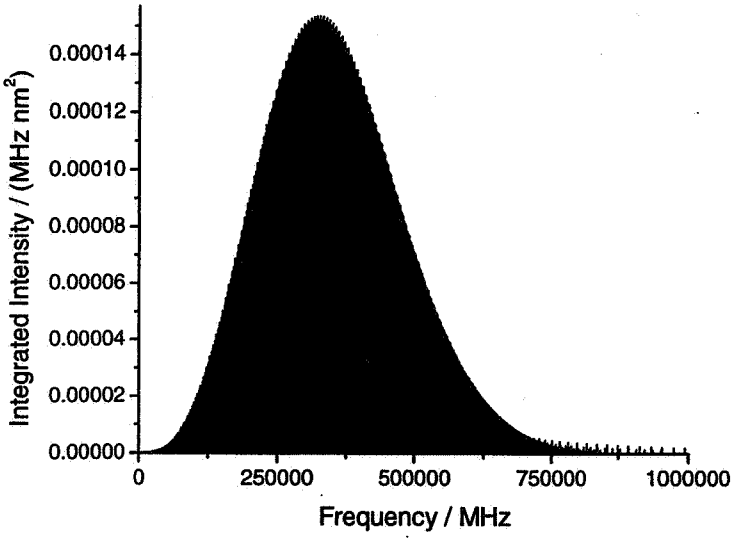

Fig. 3. Stick spectrum for the ground vibrational and conformational state of DMMP.

To determine the sensitivity requirement for detection of DMMP, we consider the most intense lines predicted in the spectrum. A set of four lines, $58_{58,1}$-$57_{57,1}$, $58_{58,0}$-$57_{57,0}$, $58_{58,0}$-$57_{57,1}$, and $58_{58,1}$-$57_{57,0}$, near 327 GHz are predicted to overlap to better than 1 kHz, and have a total intensity of 3.33×10^{-4} MHz nm^2, dominated by the two equal-intensity c-type lines ($58_{58,1}$-$57_{57,1}$, $58_{58,0}$-$57_{57,0}$), whose intensities exceed the equal-intensity b-type lines ($58_{58,0}$-$57_{57,1}$, and $58_{58,1}$-$57_{57,0}$) by the ratio of $(\mu_c/\mu_b)^2$.

This theoretical integrated intensity of 3.33×10^{-4} MHz nm^2 will be significantly smaller when the presence of other vibrational and conformational states are considered. In the absence of any tunneling processes, the intensity will be reduced by $2 \cdot (Q_{con\text{-}vib})^{-1} = 0.052$ %, where the factor of 2 allows for the fact that both enantiomers of the ground state will have identical spectra. The resulting integrated intensity is 1.73×10^{-7} MHz nm^2 (0.00560 MHz Torr^{-1} m^{-1}). For a pressure broadening coefficient of 375 kHz/Pa (50 MHz Torr^{-1}), the resulting peak absorption coefficient of the line is 1.12×10^{-4} m^{-1} for pressures greater than approximately 0.48 Pa (3.6 mTorr). In the BWO measurements discussed below a sample cell of nearly 4 m optical pathlength was

used, giving a theoretical peak absorbance of $\ln(I_0/I) = 4.5 \times 10^{-4}$ or fractional absorption of 0.045 %.

Experimental measurements (Suenram *et al.*, 2002) in concert with theoretical studies (Ohashi *et al.*, 2002, 2003) reveal that the spectroscopy of DMMP is further complicated by tunneling between the large number of equivalent minima. This tunneling lifts the degeneracies of the energy levels corresponding to the distinct configurations, splitting the absorption lines into multiplets and potentially reducing the peak absorbance.

To assess the effects of these splittings on the line intensities, we ignore, at first, tunneling of the methyl group attached to the phosphorous, which has a high barrier to internal rotation. The remaining three tunneling motions, internal rotation of the other two methyl tops and interchange tunneling exchange of the roles of the two methoxy groups, potentially split each rotational-vibrational level of a non C_s symmetry form of DMMP into eight components (2A+4E+2G) and each rotational-vibrational level of a C_s symmetry form, where the interchange tunneling is no longer possible, into four components (A+2E+G). From observations at microwave frequencies (11 GHz to 12 GHz), we expect these splittings to be resolved for measurements at Doppler-limited or better resolution in the submillimeter and THz regions. We note that interchange tunneling between the two enantiomers is possible, and, indeed, is observed at microwave frequencies. This tunneling lifts the degeneracy of the rotational-vibrational levels of the two enantiomers.

In calculating the relative intensities when the microwave-observed tunneling persists into the submillimeter, we use the relative statistical weights of 2, 4, and 8 for levels of E, A, and G symmetry respectively. Consideration of these splittings gives a peak absorbance of 1.1×10^{-4} or a fractional absorption of 0.011 % for the strongest lines in the DMMP spectrum. To measure such a small absorption coefficient requires that the BWO system be capable of detecting a change in the transmitted power through the sample cell of approximately a factor of 10 less, or of 10^{-5} or 0.001 %. We note that the signal strength is reduced by an additional factor of 2 if the splittings from the tunneling of the methyl group attached to the phosphorous are resolved.

B. Atmospheric Pressure Samples

The goal of modeling the submillimeter and THz spectrum of a chemical agent in air at atmospheric pressure is to assess the sensitivity of these spectral windows for the detection and unambiguous identification of the agent in its ambient environment. Such ambient detection methods are desired since they are rapid and do not require additional equipment for sample preparation. Also, they are potentially more accurate since the sample handling is minimized, protecting against contamination or agent loss.

At atmospheric pressure, individual rotational lines of DMMP and most of the other chemical-warfare agents are not spectrally resolved since the mean spacing between lines is significantly smaller than the pressure-broadened linewidths. The absence of spectrally resolvable features allows a number of approximations to be made to simplify the

calculation of the absorption profile, without causing a significant loss in accuracy. Estimates of the low-order moments of the spectrum and the peak fractional absorption of the radiation are of greatest interest to assess the detection sensitivity and spectral uniqueness for species identification.

Here, we will assume that the simulant, DMMP, is present as a trace impurity in dry air. For an assumed constant foreign-gas broadening coefficient of 75 kHz/Pa (10 MHz/Torr) FWHM, the pressure broadening widths will be 7.6 GHz, or approximately twice the value of the rotational constant sum, $B + C$, which specifies the spacing between the $\Delta J = 1$, $\Delta K_a = 0$, rotational progressions in the prolate symmetric-top limit. At atmospheric pressure, rotational line splittings due to tunneling can be neglected as they will be completely unresolved. We also assume that the electric dipole moments and rotational constants change little between vibrational states of the same conformer, relative to the changes in these parameters between different conformers. With these assumptions, only knowledge of the relative populations of the three conformers is necessary, and not of the individual vibrational-conformational states. These relative populations are given by the following expressions:

$$f_I = 2\, Q_{vib}^{\,I} / Q_{con\text{-}vib}$$

$$f_{II} = Q_{vib}^{\,II} \exp(-E_{II}/k_b T) / Q_{con\text{-}vib} \qquad (4)$$

$$f_{III} = 2\, Q_{vib}^{\,III} \exp(-E_{III}/k_b T) / Q_{con\text{-}vib}\,.$$

Using the constants from Table I and assuming a temperature of $T = 298.15$ K, we determine $f_I = 0.654$, $f_{II} = 0.323$, and $f_{III} = 0.023$. The relative contributions of the individual conformers to the total rotational band strength are given approximately by $f_I\mu_I^2 : f_{II}\mu_{II}^2 : f_{III}\mu_{III}^2 = 0.64:0.27:0.09$. Here, $\mu^2 = \mu_a^2 + \mu_b^2 + \mu_c^2$, is the square of the resultant molecular dipole moment for a particular conformer.

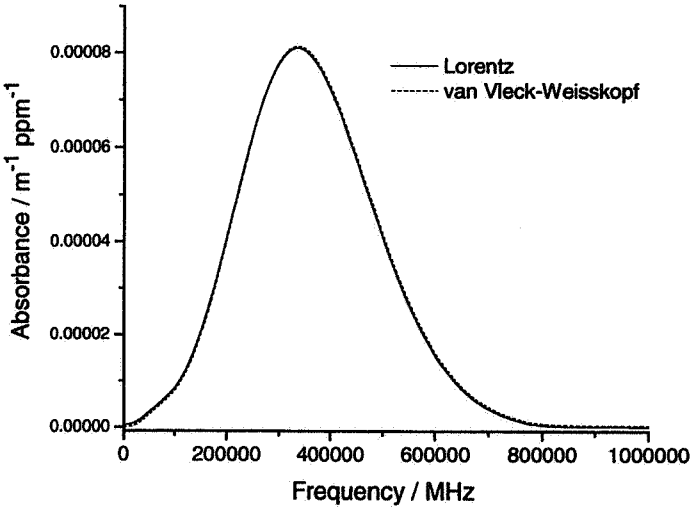

Fig. 4. Simulated spectrum of DMMP in air at 1 atmosphere total pressure (101 kPa). The log base *e* absorbance is given per m pathlength per ppm of DMMP in air. Calculations are shown for both the Lorentz and more exact van Vleck-Weisskopf collisional lineshape models.

In Fig. 4 two simulations of the DMMP spectrum are presented. The simulations were generated by summing the rotational contours from the three conformers using the f_I, f_{II}, and f_{III} weighting functions. Two collisional lineshape functions are considered for the many of thousands of individual line profiles summed to generate a rotational contour. These functions are a pure Lorentzian profile,

$$S_L(\nu) = \frac{1}{\pi}\left[\frac{\gamma}{(\nu-\nu_0)^2+\gamma^2}\right] \tag{5}$$

and the more exact van Vleck-Weisskopf profile,

$$S_{vVW}(\nu) = \frac{1}{\pi}\left(\frac{\nu}{\nu_0}\right)\left[\frac{\gamma}{(\nu-\nu_0)^2+\gamma^2} + \frac{\gamma}{(\nu+\nu_0)^2+\gamma^2}\right]. \tag{6}$$

which appropriately forces the intensity to vanishes as the frequency goes to zero. The difference between the two resulting rotational contours is negligible compared to the uncertainties in the rotational contours resulting from the unknown uncertainties in the values of the spectroscopic constants.

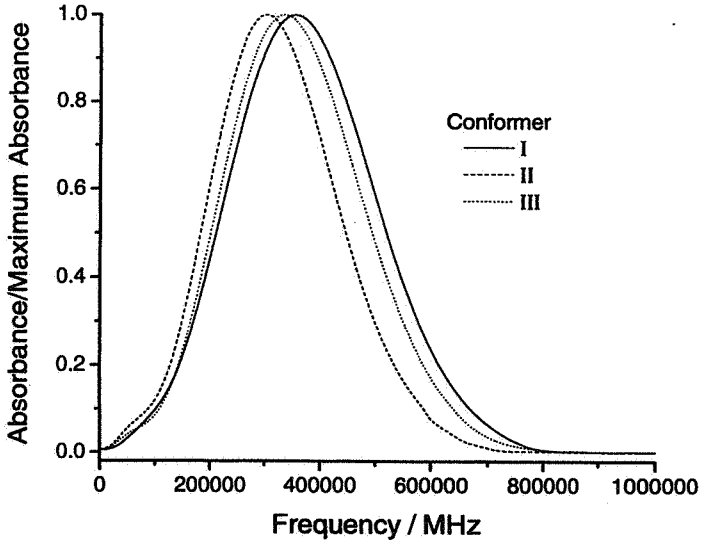

Fig. 5. Normalized rotational band contours for the three lowest-energy conformers of DMMP.

To identify a specific agent from a rotational contour such as pictured in Fig. 4 requires that the contour be relatively unique and not severely overlapped by spectral features from other background gases. As long as the background absorptions are not saturated they can, in principle, be removed by subtracting a suitable background trace, unless, of course they appear simultaneous with an agent release. To provide insight into the uniqueness of the spectral absorptions we show in Fig. 5 the rotational contours for conformers I, II, and III of DMMP, as calculated from the spectroscopic constants discussed above. We also summarize in Table II, the spectral moments, M_0, (M_1/M_0), and

$(M_2/M_0)^{1/2}$, which give the integrated band intensity, the center of gravity of the contour, and the spectral width. Despite the relative similarity of the three conformers in that they are all derived from DMMP, the moments are sufficiently distinct to suggest that band contour measurements can provide a positive identification of a chemical agent. Generally, the differences in the rotational constants between chemical agents will be greater than between conformers of the same agent.

Table II. Spectral moments for the three conformers of DMMP ignoring vibrational and conformational contributions.

Confomer No.	M_0 / (MHz nm^2)	(M_1/M_0)/ GHz	$(M_2/M_0)^{1/2}$ / GHz
I	1.09	375	131
II	0.79	326	117
III	4.00	359	126

III. Experimental Measurements

Experimental measurements were performed with a Fourier-transform far-infrared spectrometer, a laser-pumped, solid-state photomixer, and a backward-wave oscillator. As shown below, the spectrally broad and relatively structureless rotational contours present under ambient atmospheric conditions for many chemical agents are most optimally studied by lower-resolution Fourier-transform methods.

Typically, measurements were performed at the saturated room-temperature vapor pressure of DMMP by evaporating the liquid sample into a previously evacuated sample cell, and filling, when necessary, with dry nitrogen. Unfortunately, significant discrepancies exist on the vapor pressure of DMMP, with quoted values ranging from less than 13 Pa to 130 Pa (0.1 Torr to 1 Torr). Measurements made as part of the present study using thermistor and baratron pressure gauges indicate the DMMP vapor pressure is between (0.15 Torr and 0.67 Torr).

Alternatively, we have estimated the DMMP vapor pressure by a mass-loss method by evaporating a known mass of liquid DMMP into a sample cell of known volume. It was found that 230 mg of DMMP was required to fill a 50 liter cell to its saturated room-temperature vapor pressure. Assuming that the vapor behaves as an ideal gas yields a vapor pressure of 95 Pa (0.71 Torr). Possible sources for the discrepancies between the various vapor pressure measurements include temperature variation, sample condensation, high-vapor-pressure sample impurities, and vacuum leaks. The contribution of these error sources to an individual vapor pressure measurement will vary with the type of measurement and the style of vacuum or pressure gauge used. It is tempting to accept the lowest pressure literature measurement, which gives a vapor pressure of < 13 Pa (0.1 Torr), as being most correct since most of the sources of error will yield a reading which is too high. We note that our spectroscopic measurements presented below support a vapor pressure for DMMP on the order of the Material Safety Data Sheet value of < 13 Pa (0.1 Torr). Acceptance of the MSDS vapor pressure for DMMP implies that the commercial sample used in the present study suffers from

contamination by a high-vapor-pressure impurity. A more detailed investigation of the DMMP vapor-pressure is beyond the scope of the present work, but further mass-loss measurements would be valuable with a high-integrity seasoned vacuum system and a DMMP sample purified by chromatography.

A. Fourier-transform measurements

Measurements were made using a Model 45400 Fourier-transform polarizing interferometer manufactured by Graseby Specac, Inc. [†] and operating in the Martin-Puplett configuration for optimized performance between 5 cm^{-1} and 200 cm^{-1}. The instrument has a best spectral resolution of 0.025 cm^{-1}. Unique features of the instrument relative to other Fourier-transform spectrometers include the following:

- An interferometer mirror controlled by a mechanical stepping drive with a minimum step size of 1.25 μm.
- A mercury-arc lamp as a source of far-infrared radiation.
- A sample compartment optimized for measurements of transmittance, absorbance, and reflectance of solid samples.
- An evacuated optical path to reduce or eliminate water-vapor absorption.
- A modular design for maximum flexibility. The modular design requires a large number of vacuum seals, increasing the potential for leaks.
- A wire-grid beam splitter.
- A liquid-He-cooled bolometer detector.

i. 28 cm single-pass cell

Initial attempts to record the spectrum of DMMP vapor using a 28 cm long cell fitted into the sample compartment of the interferometer were unsuccessful. Such a negative result is not surprising given the relatively low vapor pressure of DMMP. Indeed, the modeling calculations above give a peak absorption coefficient of 8.1×10^{-5} m^{-1} ppm^{-1} for DMMP in 101 kPa (1 atm) air, which corresponds to a maximum fractional absorption of 0.3 % for a vapor pressure of 13 Pa (0.1 Torr). Note that here and elsewhere we are making the approximation that the absorbance, $\ln(I_0/I)$, is approximately equal to $(I_0 - I)/I_0 \equiv \Delta I/I_0$ for small absorbances, where I_0 is the detected light intensity without sample and I is the detected light intensity with sample, ignoring changes in the optical system, such as alignment, from introduction of the sample.

The 0.3 % fractional absorption, $\Delta I/I_0$, is significantly smaller than the instrument detection sensitivity of 1 % to 2 % fractional absorption in the submillimeter and THz spectral regions. We note that the above cell was successfully used for detection of water vapor in air. The spectrum shown in Fig. 6 indicates the absence of strong water-vapor absorption peaks below 18 cm^{-1} where the DMMP rotational spectrum is predicted.

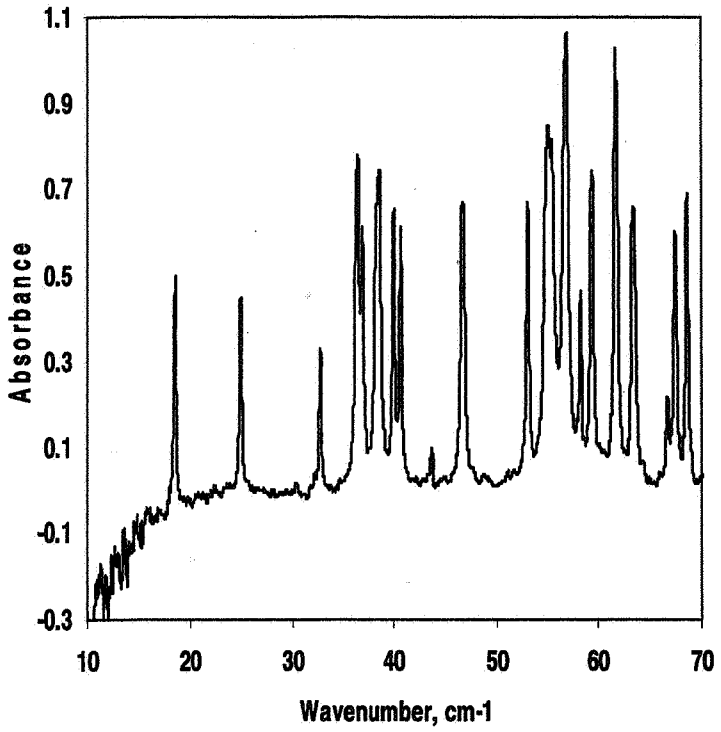

Fig. 6. Absorbance spectrum of water vapor in air under normal atmospheric conditions. Cell pathlength is 28 cm.

ii. 2 m path

Improvements in detection sensitivity for DMMP were achieved by increasing the optical pathlength by a factor of 7 to approximately 2 m and by adding a low-pass optical filter ($\lambda_{cutoff} \approx 100$ cm^{-1}) in front of the detector to reduce noise from background short-wavelength radiation. The instrument sensitivity under these conditions was assessed by recording sequentially and under identical conditions two far-infrared spectra with no sample in the optical path. Taking the ratio of the two spectra provides a measure of the system noise and thus the minimum detectable absorbance, which equals the fractional absorption of the radiation in the small absorbance limit. Such a spectral ratio is shown in Fig. 7. The minimum detectable fractional absorption is several percent at low and high wavenumbers, and as little as 0.5 % in the mid-wavenumber region.

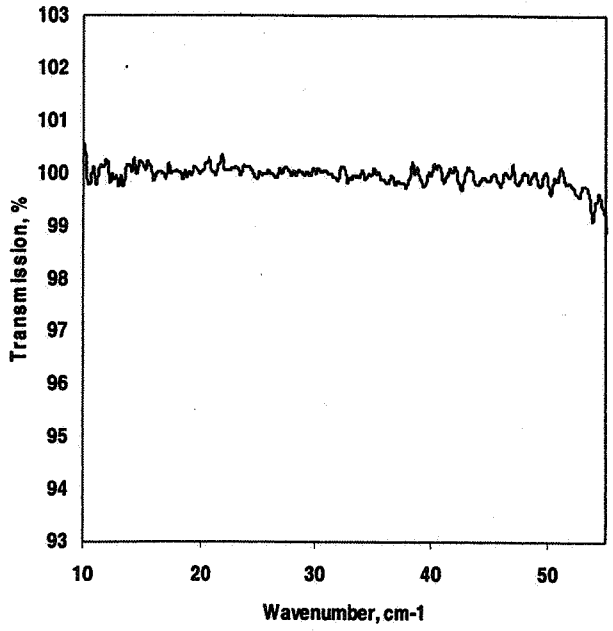

Fig. 7. A no-sample spectrum obtained from the ratioing of two vacuum traces.

A spectrum of DMMP vapor obtained with a 2 m optical pathlength are shown in Fig. 8. The sensitivity at this pathlength and with the new optical filter is sufficient to observe the rotational band contour of DMMP. Typical spectra have an absorption maximum centered between 12 cm^{-1} and 14 cm^{-1} (360 GHz and 420 GHz) and a FWHM band contour width of approximately 10 cm^{-1} (300 GHz). The magnitudes of both the absorption maximum and the band contour width are consistent with the theoretical estimates presented above.

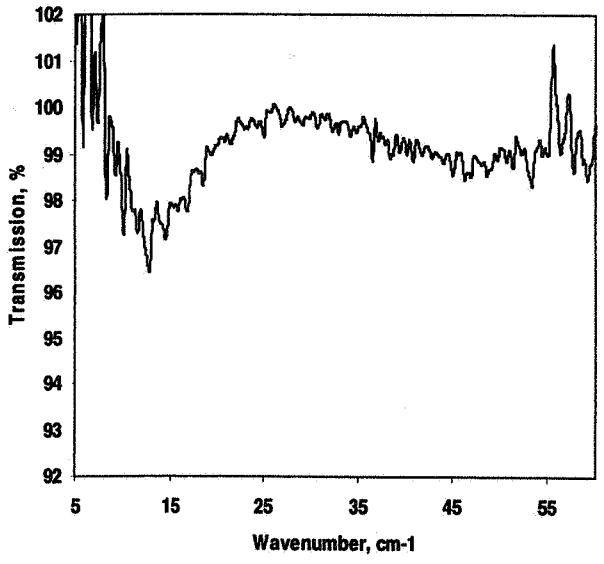

Fig. 8. Transmission spectrum of DMMP saturated vapor for an optical pathlength of 2 m.

The maximum observed absorbance is approximately, $\ln(I_0/I) \cong \Delta I/I_0 \cong 3$ %, which is slightly greater than the value of 2 % predicted from the modeling calculations for an

assumed 13 Pa (0.1 Torr) vapor pressure of DMMP. This discrepancy could be attributed to a slightly higher DMMP vapor pressure than the Material Safety Data Sheet value of < 13 Pa (0.1 Torr) at 293 K or to sample contaminants contributing to the signal.

iii. Multipass cell tests

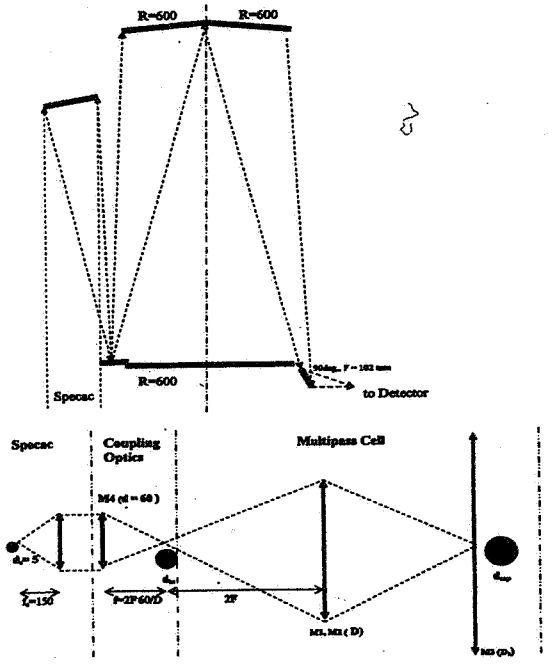

Fig. 9. Optical design of the submillimeter-to-THz multipass cell for use with the Fourier-transform spectrometer.

A White-type multipass cell is being developed to increase the sensitivity for detection of DMMP by far-infrared Fourier-transform spectroscopy. The cell is shown schematically in Fig. 9. The cell has an input aperture of approximately 60 mm and uses high-aperture f/2 optics to minimize diffraction losses in the THz to submillimeter spectral region. The optical pathlength is limited by the relatively large initial source image in this spectral region to an effective pathlength of 25 m to 35 m at 10 cm^{-1}(300 GHz).

A prototype multipass cell was tested against a 28 cm single-pass cell, with the multipass cell operating in open air since no vacuum system was yet constructed. Absorption spectra of the ambient laboratory water vapor are shown in Fig.10. The bottom trace is for the single-pass cell while the upper trace is for a multipass cell operating at approximately 22 m pathlength. In both spectra 3 strong water-vapor absorption peaks near 18 cm^{-1}, 25 cm^{-1}, and 33 cm^{-1} are observed. The increased sensitivity present in the upper longer-pathlength trace allows the observation of additional water-vapor absorption peaks near 12.6 cm^{-1}, 14.8 cm^{-1}, 15.7 cm^{-1}, 20.5 cm^{-1}, and 30.2 cm^{-1}. Note that the signal-to-noise ratio as well as the dynamic range in the upper spectrum will improve with normalization by a reference background trace, which is presently not available. The

increased pathlength available in the upper trace will also lead to possible interference of water vapor absorptions with the DMMP rotational contour. This interference may reduce the signal-to-noise ratio and therefore the detection limits for DMMP under field conditions, depending on the saturation levels.

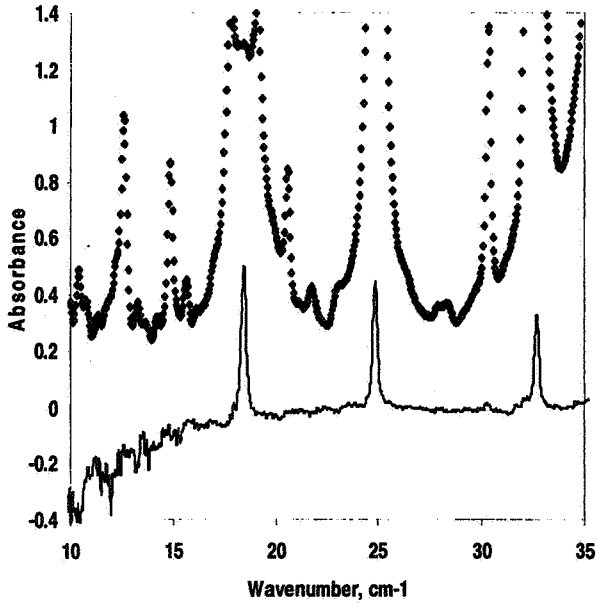

Fig. 10. Comparison of the performance of a 28 cm cell (bottom trace) against a multipass cell (top trace) for air. All absorption peaks are assigned to atmospheric water vapor.

B. Absorption measurements with photomixer system

Tunable continuous-wave submillimeter and THz radiation is generated by difference-frequency mixing the near-infrared radiation from single-mode frequency-tunable

Ti:Sapphire and fixed-frequency diode lasers, both operating near 855 nm and separated by the submillimeter or THz frequency of interest. The radiation is mixed in a solid-state GaAs photomixer consisting of a GaAs wafer onto which is grown an epitaxial thin film of low-temperature-grown GaAs (LT-GaAs). The LT-GaAs layer is topped by submicron interdigitated gold-on-titanium electrodes, which are coupled to a self-complementary spiral antenna for broad-band output. The photomixer has an 8 μm × 8 μm central region containing eight 8 μm x 0.2 μm electrodes separated by 0.8 μm, which is illuminated by the two coaxial laser beams. The front surface of the photomixer is antireflection coated. The photomixer is operated at room temperature and biased with a voltage of 15 V to 20 V. The output radiation from the photomixer is collimated by a 2.54 cm diameter Si hyper-hemispherical lens.

After exciting the Si lens the radiation is further collimated by a Teflon or high-density polyethylene lens so that ≈ 80 % of output power is available for detection after propagation through a 1 m long sample cell. The detector is a high-sensitivity, liquid-He-cooled, Si composite bolometer. The power at the detector input is approximately 300 nW, dependent on frequency. The near-infrared radiation is chopped at 300 Hz for

phase-sensitive detection. The photomixer spectrometer was tested for detection limits in two different operational modes:

- Low Resolution (LR) mode with a spectral resolution of ≈ 0.1 cm^{-1} and wide single-scan coverage from 2 cm^{-1} to 140 cm^{-1}.
- High Resolution (HR) mode with a spectral resolution of $\approx 3 \cdot 10^{-5}$ cm^{-1} and narrow 0.75 cm^{-1} single-scan overage in the range from 2 cm^{-1} to 140 cm^{-1}.

The low-resolution mode is appropriate for atmospheric pressure samples were rotational structure is not resolvable, while the high-resolution mode is used for the investigation of low-pressure samples where individual lines or clumps of lines could potentially be resolved.

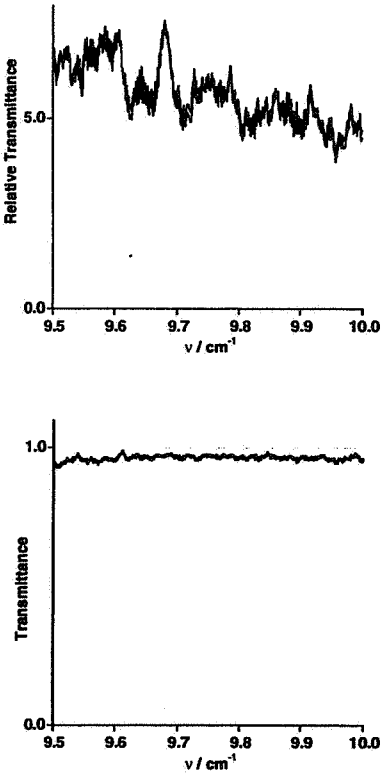

Fig. 11. Low-resolution photomixer spectra of a 37 Pa (0.28 Torr) sample saturated with DMMP vapor in a 1 m cell. The average fractional absorption of 3(1) % over the 0.5 cm^{-1} range is greater than the baseline reproducibility and is consistent with the maximum fractional absorption expected for DMMP as estimated from the modeling and Fourier-transform studies.

i. High-Resolution Measurements

Initial measurements were performed in High Resolution (HR) mode because of the anticipated increase in peak absorption intensity for individual DMMP rotational lines. For a total sample pressure of 37 Pa (0.28 Torr), an assumed partial pressure of DMMP of 13 Pa (0.1 Torr), and foreign and self-broadening coefficients of 0.075 MHz/Pa (10 MHz/Torr) and 0.375 MHz/Pa (50 MHz/Torr), respectively, a FWHM linewidth of approximately 7 MHz is estimated, which should be resolvable in HR mode where the THz linewidth is approximately 3 MHz to 5 MHz. Several 20 GHz spectral windows were scanned between 4 cm^{-1} and 20 cm^{-1} to search for individual rotational or rotational-

tunneling lines. A typical 20-GHz trace is presented in Fig.11. Even though this method provides for excellent discrimination against anomalous features such as "etaloning", no reproducible sharp structure was found that could be assigned to DMMP at the level of 1 percent or more. However, the average fractional absorption of 3(1) % over the 0.5 cm^{-1} range is larger than the estimated baseline reproducibility of 1 %, as determined by repeated measurements of vacuum and DMMP spectra. This small baseline shift is consistent with the maximum fractional absorption of ≈ 2 % expected for a 13 Pa (0.1 Torr) vapor-pressure sample in a meter-long cell assuming no tunneling splittings are resolved.

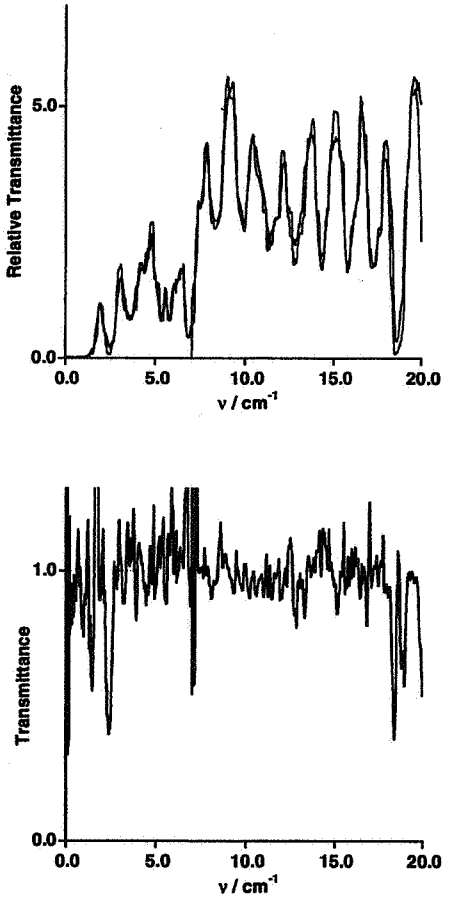

Fig. 12. Low-resolution photomixer survey scans of nitrogen gas saturated with DMMP vapor in a 1 m long optical cell. The baseline measurement reproducibility of 5 % to 10 % in fractional absorption limits the ability to observed the smaller 2 % fractional absorption expected for DMMP.

ii. Low-Resolution Measurements

Scans were also performed in LR mode to rapidly cover a much broader frequency range, here from 2 cm^{-1} to 20 cm^{-1}. Data were obtained for the DMMP vapor and for DMMP vapor added to 101 kPa (1 atm) of nitrogen. As illustrated in Fig 12, the slight frequency deviations in the reproducibility of the scans severely limit the fractional absorption sensitivity of this technique to 5% to 10 %. At this level of sensitivity, no absorption was detected which could be attributed to DMMP.

C. Backward Wave Oscillator measurements

Backward-wave oscillator (BWO) measurements were performed to assess the potential of detecting the DMMP rotational structure under conditions were individual rotational lines are resolvable. Measurements were performed between 234 GHz and 237 GHz where a number of rotational lines are predicted. The BWO instrument was operated in both AM- and FM-modes, with the FM sensitivity best for narrow absorption lines. An FM modulation depth 0f 0.8 MHz and modulation frequency of $f = 50$ kHz was used for $2f$ detection with a lock-in amplifier with a 30 ms time constant. The collimated BWO radiation was directed through a 3.5 meter cell onto a liquid-He-cooled, InSb, hot-electron bolometer detector.

The cell had a base pressure of 0.4 Pa (3 mTorr) and was operated at vapor pressures from 13 Pa to 80 Pa (100 mTorr to 600 mTorr) from the DMMP sample, as determined from a capacitance manometer. System sensitivity was tested on SO_2, for which the absolute submillimeter absorption cross sections are known and tabulated by Pickett *et al.* (1991). In Fig. 13 a spectral trace of a 6.3 Pa (47 mTorr) sample of SO_2 is shown in the 3.5 m cell using FM modulation. The weaker line has a tabulated integrated absorption coefficient of 5.1×10^{-5} MHz nm^2. At 6.3 Pa (47 mTorr) and a 3.5 m pathlength the weak line near 226508 MHz has a peak absorbance of 0.79 for a Doppler limited lineshape and 0.15 assuming a pressure broadening coefficient of 0.15 MHz/Pa (20 MHz/Torr) HWHM. Dividing these absorbances by the observed signal-to-noise ratio (S/N) of the line provides an estimate of the minimum detectable absorbance. The noise in the spectrum has both a coherent component, due to standing wave structure, characterized by a $S/N \approx 2$, and a smaller random component, characterized by a $S/N >$ 2000. The effective S/N is between these two values, and is estimated as approximately 100, giving minimum detectable absorbances between 0.0015 and 0.0079, or a minimum detectable fractional absorption between 0.15 % and 0.79 %.

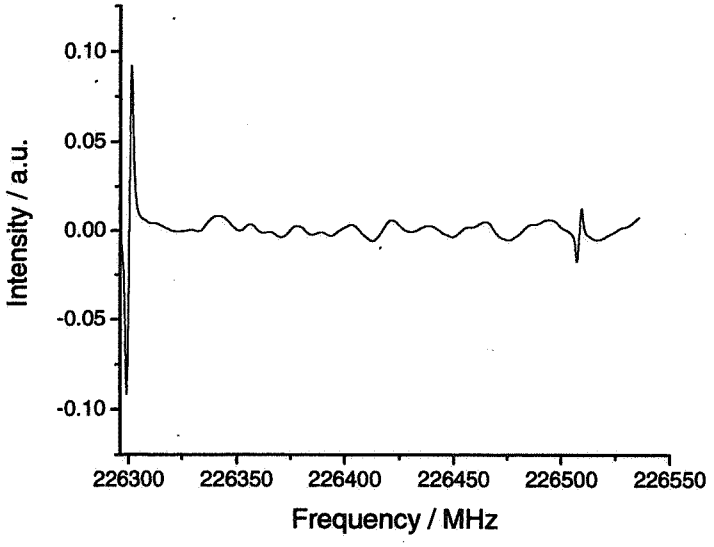

Fig. 13. BWO spectrum of SO_2 to assess system sensitivity. The ripple baseline is attributed to standing wave structure from the various transmissive optical components.

The theoretical modeling indicates that a sensitivity of approximately 0.001 % in fractional absorption is required to observe DMMP lines in high resolution. An improvement in detection sensitivity by at least 150 is thus necessary. To achieve such a sensitivity improvement should be possible by improving the optical system to reduce the standing wave structure primarily limiting the detection sensitivity. Optical system design improvements include using mirrors instead of lens, operating in a narrow frequency window to allow the use of antireflective coatings, and developing software algorithms to model the baseline. Additionally, the system time constant could be increased by a factor of 100 to 300 ms, reducing random noise by a factor of 10. Additional efforts need to be made at improving the quality of the DMMP sample and the vacuum system to allow operation at the low pressures necessary for Doppler-limited resolution (Pressure = 0.48 Pa or 3.6 mTorr). This Doppler-limited resolution provides the greatest discrimination between the relatively broad baseline-standing wave structure and the sharp DMMP lines.

IV. Conclusion

The present study has addressed the detection of chemical-warfare agents with continuous-wave submillimeter and THz spectroscopies at low and high spectral resolutions. Only the low-resolution methods offer an opportunity for a field detector, in that they can operate with atmospheric-pressure samples. The high-resolution methods, on the other hand, should improve our understanding of the spectral, structural, and dynamical properties of chemical agents, important for generating spectral models and for validating computational and molecular mechanical models of the agents used in material properties calculations, kinetic modeling, biochemical studies, and sensor development.

As shown above, the low-resolution Fourier-transform measurements have observed the rotational band contour for DMMP, a nerve agent simulant. An effort to improve the detection sensitivity by an order of magnitude is expected upon completion of a compact, long-pathlength, multipass cell. High-resolution photomixer studies also show a baseline offset from the presence of DMMP which is attributed to broadband absorption by the collisionally broadened rotational band contour. Attempts at observing DMMP lines at low resolution with the photomixer were challenged by the expected small fractional absorptions and the relatively low sensitivity of the spectrometer in this operational mode, primarily due to the baseline standing-wave structure.

In principal the BWO has the capability of observing DMMP at high spectral resolution, however, the present instrument needs significant improvements to achieve this goal, driven by the small fractional absorptions expected. In particular, efforts are required to eliminate the "noise" arising from standing-wave structures by reducing the number of transmissive optics and by developing improved baseline models for removal of this noise. The actual noise at a fixed frequency is small, on the order of 1000 times less than the baseline fluctuations, and is theoretically the limiting noise source in the experiment. Unfortunately, much of the dynamic range of the detection system is wasted capturing the large baseline drifts. An additional effort needs to be made to further purify the DMMP

sample and ensure the integrity of the vacuum system to allow operation of the instrument at extremely low pressures, on the order of fractions of a Pa (several mTorr), necessary to ensure the highest spectral resolution.

References

† Certain commercial equipment, instruments, or materials are identified in this paper to specify the experimental procedure adequately. Such identification is not intended to imply recommendation or endorsement by the National Institute of Standards and Technology, nor is it intended to imply that the materials or equipment identified are necessarily the best available for the purpose.

B.N. Taylor and C.E. Kuyatt, "Guidelines for Evaluating and Expressing the Uncertainty of NIST Measurement Results," NIST Technical Note 1297, (U.S. Government Printing Office, Washington, D.C., 1994). Also available by the internet at http://physics.nist.gov/Document/tn1297.pdf

L. Zu, P. A. Hamilton, and P. B. Davies, "Pressure broadening and frequency measurements of nitric acid lines in the 683 GHz region," *J. Quant. Spectros. Rad. Trans.* **73**, 545-556 (2002).

R. D. Suenram, F. J. Lovas, D. F. Plusquellic, A. Lesarri, Y. Kawashima, J. O. Jensen, and A. C. Samuels, "Fourier Transform Microwave Spectrum and *ab initio* Study of Dimethyl Methylphosphonate," *J. Mol. Spectrosc.* **211**, 110-118 (2002).

N. Ohashi and J. T. Hougen, "Application of Permutation-Inversion Group Theory to the Interpretation of the Microwave Absorption Spectrum of Dimethyl Methylphosphonate," *J. Mol. Spectrosc.* **211**, 119-126 (2002).

N. Ohashi, J. Pyka, G. Yu. Golubiatnikiov, J. T. Hougen, R. D. Suenram, F. J. Lovas, A. Lesarri, and Y. Kawashima, "Line Assignments and Global Analysis of the Tunneling-Rotational Microwave Absorption Spectrum of Dimethyl Methylphosphonate," *J. Mol. Spectrosc.* 2003. (to be published).

H. M. Pickett, "The Fitting and Prediction of Vibration-Rotation Spectra with Spin Interactions," *J. Molec. Spectroscopy* 148, 371-377 (1991). (see: http://spec.jpl.nasa.gov/)

C. H. Townes and A. L. Schawlow, *Microwave Spectroscopy*, (McGraw-Hill, New York, 1955)